Hindawi Publishing Corporation
Journal of Crystallography
Volume 2014, Article ID 585282, 8 pages
http://dx.doi.org/10.1155/2014/585282

Research Article

Quantitative Crystal Structure Analysis of (*E*)-1-[(2-Chloro-1,3-thiazol-5-yl)methyl]-3-methyl-2-nitroguanidine

Dhananjay Dey,[1] Chetan S. Shripanavar,[2] Kaushik Banerjee,[2] and Deepak Chopra[1]

[1] *Indian Institute of Science Education and Research Bhopal, Bhopal 462066, India*
[2] *National Research Centre for Grapes, Pune 412307, India*

Correspondence should be addressed to Deepak Chopra; dchopra@iiserb.ac.in

Received 8 January 2014; Accepted 5 March 2014; Published 15 June 2014

Academic Editor: Mehmet Akkurt

The crystal structure of a biologically active (*E*)-1-[(2-chloro-1,3-thiazol-5-yl)methyl)]-3-methyl-2-nitroguanidine with molecular formula $C_6H_8N_5O_2ClS$ has been investigated based on the molecular conformation and the supramolecular packing in terms of intermolecular interactions involving N–H···O, N–H···N, and C–H···O–N (nitro group), C–H···N (thiazol) hydrogen bonds, offset π–π stacking, C–H···π and N($-NO_2$)···C=N intermolecular interactions. Furthermore, a short C–Cl···O–N contact is also present which contributes towards the crystal packing. The lattice energy of the title compound has been calculated using the PIXEL approach (the Coulomb-London-Pauli (CLP) model) and compared with periodic calculations performed using CRYSTAL09. In addition, Hirshfeld surface analysis and fingerprint plots provide a platform for the evaluation of the contribution of different intermolecular interactions towards the packing behaviour.

1. Introduction

(*E*)-1-(2-Chloro-1,3-thiazol-5-ylmethyl)-3-methyl-2-nitroguanidine [1] constitutes a new class of neonicotinoid insecticides [2–5], which is useful to rice, leafy vegetables, tomato, and tea to control noxious insects, with excellent systemic action [6]. Clothianidin exhibits excellent control efficacies in small amounts for a wide variety of insect pests such as Hemiptera, Thysanoptera, Coleoptera, Lepidoptera, and Diptera for a long term, with excellent systemic action and by a variety of application methods [7]. The crystal structure of this title compound has been reported in 2003 [8]. It is of interest to investigate the crystal packing of the molecule in the solid state. Furthermore, an investigation of the molecular conformation in the solid state and comparison with the gas phase is also of relevance. In addition, a quantitative estimation of the energetics and nature of weak intermolecular interactions which pack the solid have also been performed. Keeping in mind the above-mentioned viewpoints we have recrystallized the compound and redetermined the crystal structure by single crystal X-ray diffraction at 100(2)K. The previous determination was performed at 153 K [8].

The total lattice energy has also been calculated and this is divided into the corresponding Coulombic, polarization, dispersion, and repulsion energies [9]. The molecular pairs (in the crystal packing) were extracted and their energies were compared with the values obtained from high level DFT + disp calculations at the crystal geometry with BSSE [10] corrections. The lattice energy obtained from the PIXEL has been compared with the value achieved from Crystal 09 [11]. Hirshfeld surfaces [12] mapped with d_{norm} using a red-white-blue colour scheme, where red is used to indicate the shorter contacts, white is used for contacts around the vdW separation, and blue is for longer contacts along with the fingerprint plots [13], have been studied to evaluate the contribution of the individual types of interaction within the crystal structures. Hirshfeld surface and fingerprint plots of the title compounds also provide the information about the different supramolecular interaction motifs. CSD search

(version 5.34 updates February 2013) also provides one result on the π–π stacking of the thiazole ring which is close to our analysed value [14].

2. Experimental

The compound was purchased from Bayer Crop Science Ltd, Mumbai. The pure compound was dissolved in methanol and crystals obtained at room temperature. The melting point of the title compound obtained from DSC is 178.20°C (Figure S1, see Supplementary Material available online at http://dx.doi.org/10.1155/2014/585282).

2.1. X-Ray Crystallography. X-ray diffraction datasets were collected on a three-circle Bruker APEX-II diffractometer equipped with a CCD area detector using Mo-Kα radiation ($\lambda = 0.71073$ Å) in φ and ω scan modes. The crystal structures were solved by direct methods using SIR92 [15] and refined by the full matrix least squares method using SHELXL97 [16] present in the program suit WinGX [17]. The nonhydrogen atoms are refined anisotropically and the hydrogen atoms bonded to C atoms were positioned geometrically and refined using a riding model with $U_{iso}(H) = 1.2U_{eq}$ (C, N) for aromatic hydrogens and $U_{iso}(H) = 1.5U_{eq}$ (C) for hydrogen atoms of the methyl group and methylene group. The molecular connectivity was drawn using ORTEP32 [18] and the crystal packing diagrams were generated using Mercury 3.1 (CCDC) program [19]. Geometrical calculations were done using PARST [20] and PLATON [21]. Powder X-ray diffraction (PXRD) data was recorded for the solid compounds and then compared with the simulated PXRD patterns generated from the crystal coordinates in Mercury 3.1 and the final plot was drawn in OriginPro 8. The details of the crystal data, data collection, and structure refinements are shown in Table 1. Hirshfeld surfaces and the associated 2D-fingerprint plots were generated using Crystal Explorer 3.0 [22].

2.2. Theoretical Calculations. The geometrical optimization of the molecule has been performed at the B3LYP/6-31G** level of calculation using TURBOMOLE [23, 24]. The selected torsion angles of compound obtained from theoretical calculations were then compared with the solid state. DFT + Disp calculations were done with the functional B97-D using a higher basis set aug-cc-pVTZ in TURBOMOLE. The lattice energies of these crystal structures have been calculated by PIXEL using the Coulomb-London-Pauli (CLP) model of intermolecular Coulombic, polarization, dispersion, and repulsion energies. Furthermore, high level DFT + Disp quantum mechanical calculations for comparison with the pairing energies obtained from PIXEL method have been carried out.

3. Results and Discussion

Clothianidin (Figure 1) crystallizes in a centrosymmetric triclinic space group P-1 with one molecule in the asymmetric unit, thus having $Z = 2$. The molecule contains one thiazole moiety and one Cl atom. In addition, a nitroguanidine moiety is attached *via* methylene bridge of the thiazole ring. Clothianidin bears a total of five types of nitrogen with different electronic environment, among them N1 and N3 have more basic character than the other nitrogen atoms because of the lone pair of electrons present compared to N2 and N5 which are involved in resonance with the imine bond.

Table 1: Crystallographic and refinement data.

Formula	$C_6H_8N_5O_2ClS$
Formula weight	249.68
Wavelength (Å)	0.71073
Temperature (K)	100(2)
Solvent system	Methanol
CCDC number	943833
Crystal system	Triclinic
Space group	P-1
a, b, c (Å)	7.2424(3), 7.9943(3), 9.2677(4)
α, β, γ (°)	86.667(2), 79.259(2), 73.175(2)
V (Å^3)	504.61(4)
Z	2
Density (g cm^{-3})	1.643
μ (mm^{-1})	0.574
$F(000)$	256
θ (min, max)	2.83, 22.63
Treatment of hydrogens	Fixed
$h_{min,max}, k_{min,max}, l_{min,max}$	(−9, 9), (−10, 9), (−9, 12)
Number. of ref.	8323
Number of unique ref./ obs. ref.	2299, 2132
Number of parameters	137
R_all, R_obs	0.0306, 0.0283
wR_2_all, wR_2_obs	0.0755, 0.0740
$\Delta\rho_{min,max}$ (eÅ^{-3})	−0.327, 0.232
G. o. F	1.086

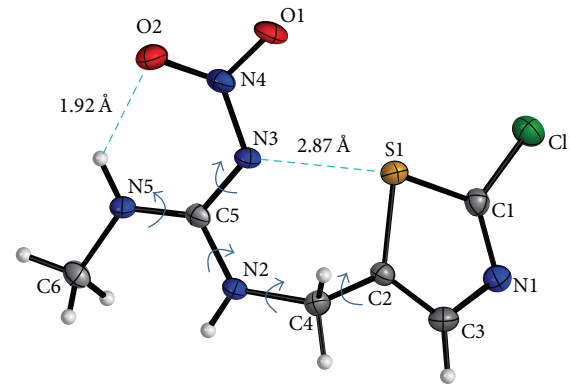

Figure 1: *ORTEP* of the title compound drown with 50% ellipsoidal probability. Bending arrows indicate the significant torsion angles in the asymmetric unit and the dotted lines designate the intramolecular hydrogen bond between amidic hydrogen (H5) and oxygen atom (O2) of the nitro group and N···S short contact.

Table 2: Selected torsion angles (°).

Torsion	Experimental	Theoretical
N2–C4–C2–C3	120.30(15)	*108.32*[a]
N4–N3–C5–N2	177.80(12)	*176.26*[a]
C4–N2–C5–N5	179.69(13)	*176.02*[a]
C6–N5–C5–N3	179.33(14)	*175.48*[a]
C5–N2–C4–C2	101.15(16)	*98.68*[a]

[a]Italicised values obtained from theoretical B3LYP/6-31G** calculation.

Table 3: Selected bond angles (°).

Bond angle	Experimental	Theoretical
C5–N2–C4	122.62(11)	*122.05*[a]
N4–N3–C5	119.20(11)	*119.72*[a]
O2–N4–N3	124.57(11)	*122.29*[a]
O1–N4–N3	114.46(12)	*115.07*[a]
C5–N5–C6	122.82(12)	*125.09*[a]
N2–C4–C2	113.73(12)	*115.00*[a]

[a]Italicised values obtained from theoretical B3LYP/6-31G** calculation.

Tables 2 and 3 list some selected torsion angles and bond angles present in the molecule, respectively. The N2–C4–C2–C3 torsion angle value differs by 12° from the theoretical value obtained after the geometrical optimization at the B3LYP/6-31G** level of calculation using TURBOMOLE. The remaining experimental torsion angles (indicated in Figure 1) are close to the theoretical values. The bond angle C5–N5–C6 differs by 2° when compared to the value obtained from the gaseous state. In Figure 2, the overlay diagram has been drawn to show the differences in molecular conformation, with the molecule in the solid state being compared with the geometry in the gas phase. The molecule is "V-shaped" the planar thiazole ring is in one plane, and the nitroguanidine moiety is in another plane (due to electron delocalisation of the lone pair of electrons of N2 and N5 over the double bond and the nitro group). The dihedral angle between the two planes is 116.16(4)°.

3.1. Crystal Packing. All the geometrically relevant intra-, intermolecular hydrogen and halogen bonds in the title compound are given in Table 4. The geometrical restrictions placed on the intermolecular H-bonds are the sum of the van der Waals radii + 0.4 Å; the directionality is greater than 110° [25]. The crystal packing of this molecule has been described *via* C–H···O, N–H···O, C–H···N, N–H···N, C–H···π [26–28], offset π–π stacking [29], Cl···O halogen bond, and N($-NO_2$)···C=N intermolecular interactions. An intramolecular short contact between N3 and S1 with a distance of 2.87 Å along with an intramolecular N–H···O hydrogen bond is present in the molecular conformation. The bifurcated acceptor N1 forms one C–H···N hydrogen bond and one N–H···N hydrogen bond (involving H5 and H6B, resp.) along the *c*-axis. Two adjacent centrosymmetric layers are connected by C–H···O hydrogen bonds (involving H6A and H6C with O2 and O1, resp.), C–H···π intermolecular interactions (involving H4B), and π–π stacking (involving the thiazole ring), alternatively (Figure 3). The assembly of molecules down the *a*-axis is held by N–H···O (involving H2 with O1) and C–H···O intermolecular H-bonds (hydrogen atoms H4A with O1 and H6C with O2 present in the nitro group) in the crystal packing (Figure 4). Two adjacent centrosymmetric layers are held by Cl···O halogen bond and π–π stacking (Figure 4). Also, the N atom (having positive charge) on the nitro group interacts with the carbon atom (C5), with the distance being 3.162(2) Å.

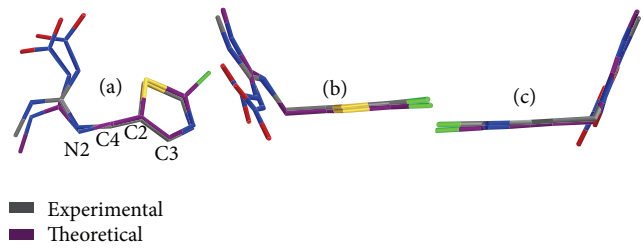

Figure 2: Overlay diagram between experimental and theoretical molecular conformations of the title compound.

Extracted molecular pairs obtained from the PIXEL calculation have been discussed in the order of decreasing interaction energy (Table 5 and Figure 4). One C–H···O (involving O1 with H6C) and N($-NO_2$)···C=N intermolecular interaction generates a molecular pair across the centre of symmetry, and the energetic stabilization is −14.7/−15.9 kcal/mole obtained from PIXEL/TURBOMOLE (Figure 5). It is of interest to note that out of the total stabilization of 20.3 kcal/mol, 45% of the stabilization comes from the Coulombic contribution. This molecular pair provides a much higher contribution towards the crystal packing compared with the other molecular pairs. Molecular offset π–π stacking (involving Cg1 with Cg1 of another molecule, where Cg1 = S1–C1–N1–C3–C2), across the centre of symmetry, also provides stabilization (energy of −11.7/−10.0 kcal/mole) towards the crystal packing. In this case, the centroid-centroid distance is 3.682 Å; the two five membered thiazole rings have a lateral displacement with respect to each other. Another molecular pair having comparable pairing energy (−11.2/−10.5 kcal/mole) with the previous one (bifurcated acceptor O1 with H2 and H4A, H6C and O2) forms a chain along the *a*-axis. The Coulombic contribution towards the total stability is 60%. Another C–H···O intermolecular interaction constructs a dimer across the centre of symmetry with an energetic stabilization of −9.7/−9.6 kcal/mole. Furthermore, H4B atom participates in a C–H···π intermolecular interaction, which generates a dimer across the centre of symmetry; the energetic stabilization is −9.4/−10.3 kcal/mole. Bifurcated acceptor N1 constructs two different hydrogen bonds (N–H···N and C–H···N) along the *c*-axis; the pairing energy is −6.2/−4.5 kcal/mole. In addition, halogen bonding also plays an important role and contributes to the crystal stability. Cl1···O1 creates a molecular dimer across the center of symmetry with less energy of −2.4/−0.3 kcal/mole. From the graphical plot (Figure 6) of the pairing energy with the centroid-centroid distance, it has been found that most of the molecular pairs with a high pairing energy obtained from the

Table 4: List of intra- and intermolecular hydrogen bonds present in the title compound.

D–H···A	D–H (Å)	D···A (Å)	H···A (Å)	∠D–H···A (°)	Symmetry
N5–H5···O2	1.03	2.613(2)	1.92	123	x, y, z
N2–H2···O1	1.03	2.844(2)	1.99	139	$x + 1, y, z$
C4–H4A···O1	1.08	3.261(2)	2.69	113	$x + 1, y, z$
C6–H6C···O2	1.08	3.432(2)	2.87	112	$x + 1, y, z$
C6–H6B···N1	1.08	3.333(2)	2.73	115	$x, y, z - 1$
N5–H5···N1	1.03	3.019(2)	2.23	132	$x, y, z - 1$
C6–H6C···O1	1.08	3.476(2)	2.73	126	$-x + 2, -y, -z + 1$
C4–H4B···O2	1.08	3.510(2)	2.84	120	$-x + 2, -y, -z + 1$
C6–H6A···O2	1.08	3.678(2)	2.76	143	$-x + 2, -y + 1, -z + 1$
C4–H4B···Cg1	1.08	3.645(2)	2.68	139	$-x + 1, -y + 1, -z + 2$
C–X···Y–N	X···Y (Å)		∠C–X···Y (°)	∠X···Y–N (°)	Symmetry
Cl–Cl1···O1–N4	3.137(11)		154	98	$-x + 1, -y + 1, -z + 2$

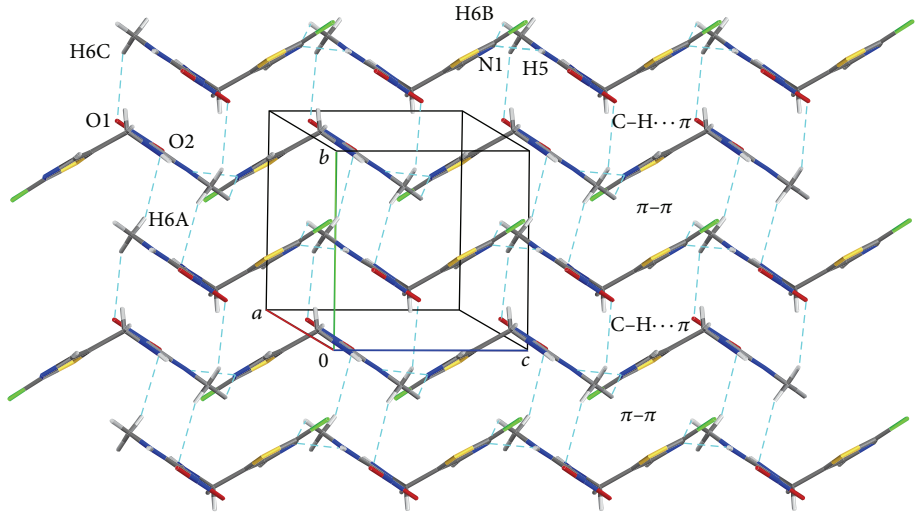

Figure 3: Crystal packing showing a zigzag arrangement of molecules, involving C–H···N, C–H···O, N–H···N, and alternate C–H···π intermolecular interactions and π–π stacking down the *bc* plane.

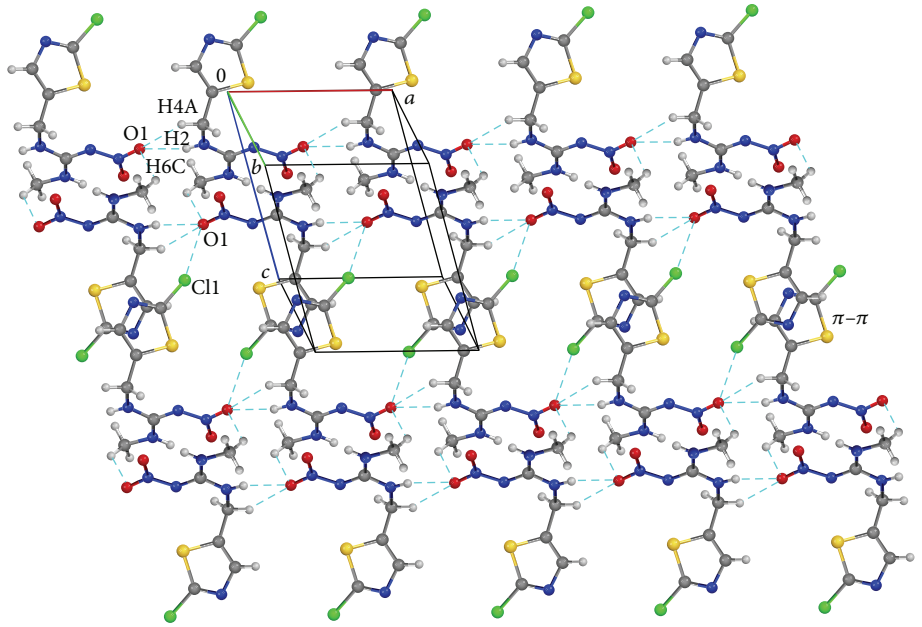

Figure 4: Crystal packing showing an array of molecules which forms a sheet containing C–H···O, Cl···O intermolecular interactions and π–π stacking down the *ac* plane.

Table 5: PIXEL interaction energies (in kcal/mol) between molecular pairs related by a symmetry operation and the associated intermolecular interactions in the crystal.

Number	Symmetry	Centroid distance	E_{Coul}	E_{Pol}	E_{Disp}	E_{Rep}	E_{Tot}	DFT-Disp/B97-D aug-cc-pVTZ	Involved interactions
A	$-x+2, -y, -z+1$	7.086	−9.1	−2.1	−9.1	5.6	−14.7	−15.9	C6–H6C···O1 C4–H4B···O2 N4···C5
B	$-x+2, -y+1, -z+2$	5.749	−5.4	−2.5	−12.0	8.2	−11.7	−10.0	Cg1···Cg1
C	$x+1, y, z$	7.242	−10.6	−3.0	−4.2	6.7	−11.2	−10.5	C2–H2···O1 C4–H4A···O1 C6–H6C···O2
D	$-x+2, -y+1, -z+1$	6.768	−4.4	−1.7	−6.3	2.7	−9.7	−9.6	C6–H6A···O2
E	$-x+2, -y, -z+2$	5.371	−4.6	−2.6	−10.5	8.3	−9.4	−10.3	C4–H4B···Cg1
F	$x, y, z-1$	9.268	−4.7	−3.0	−5.4	6.8	−6.2	−4.5	N5–H5···N1 C6–H6B···N1
G	$-x+1, -y+1, -z+2$	6.612	−0.7	−1.5	−7.0	6.7	−2.4	−0.3	Cl1···O1

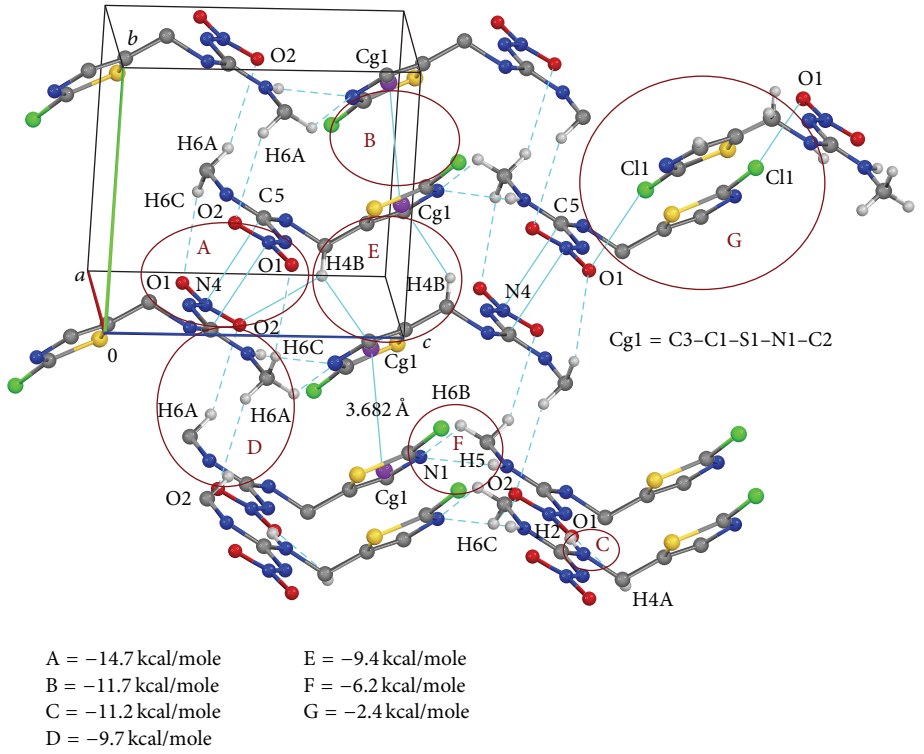

A = −14.7 kcal/mole
B = −11.7 kcal/mole
C = −11.2 kcal/mole
D = −9.7 kcal/mole
E = −9.4 kcal/mole
F = −6.2 kcal/mole
G = −2.4 kcal/mole

Figure 5: Packing diagram showing all the intermolecular hydrogen bonding (C–H···O–N, C–H···N, and N–H···N), molecular stacking (Cg1···Cg1, C–H···Cg1, N···C), and also the molecular pairs with their corresponding energies obtained from the PIXEL calculation.

Table 6: Lattice energy (in kcal/mol) of the title compound.

E_{Coul}	E_{Pol}	E_{Disp}	E_{Rep}	E_{Tot}/Crystal 09
−24.6	−9.2	−37.0	30.7	−40.1/−42.3

PIXEL calculation are observed in the region between 5.3 Å to 7.2 Å and the remaining molecular pairs with comparatively reduced stabilization energy exist at much longer distances. Table 6 lists the lattice energy obtained from PIXEL and has been compared with the lattice energy obtained from Crystal 09.

3.2. Hirshfeld Surface Analysis. The Hirshfeld surfaces of this compound are described in Figure 7, showing surfaces that have been mapped over d_{norm} (−0.5 to 1.5 Å). The large circular depressions (deep red) visible on the front view and the back view of the surfaces are indicative of hydrogen-bonding contacts. The other visible colour spots are observed due to the presence of other close contacts

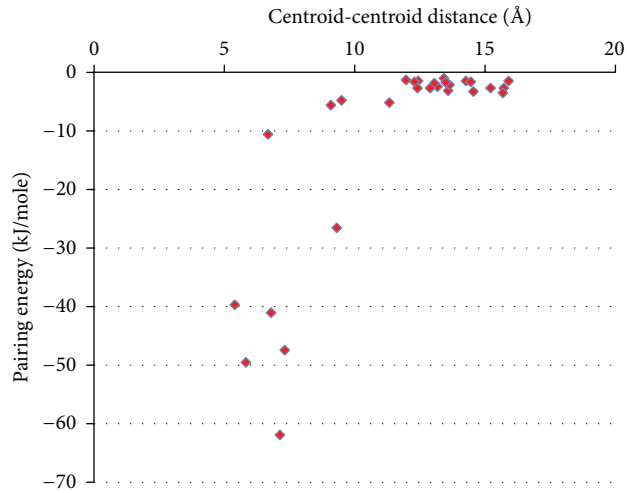

Figure 6: Graphical plot of pairing energies present in the crystal packing with the centroid-centroid distance obtained from the PIXEL calculation.

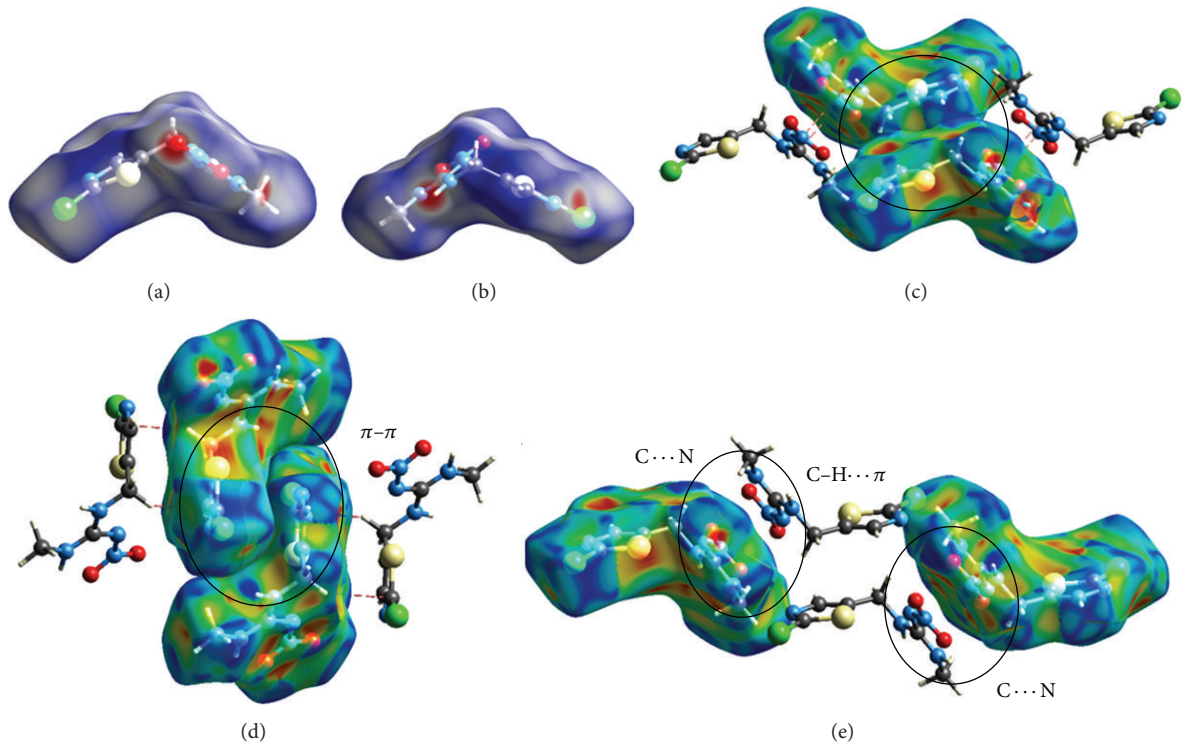

Figure 7: Hirshfeld surfaces mapped with (a) d_{norm} of front view and (b) d_{norm} of back view and (c), (d), and (e) showing the shape index for the selected molecular pairs of the title compound.

like H···H, C···H, and C···C. In the d_{norm} plot for the front view, a deep red spot indicated the presence of a N–H···N hydrogen bond (between N1 and H5) and the middle deep red spot depicted the presence of a C–H···O hydrogen bond (between O1 and H2) (Figure 7(a)). Similarly, in the back view for the d_{norm}, the left side spot is for the interaction of O1 with H2 and the right side spot is for the interaction of N1 with H5 (Figure 7(b)). Figure 7(c) shows the shape index of the molecular pair having C–H···π hydrogen bonding with H4B. In the shape index, red and blue triangles indicate the presence of molecular stacking. Figure 7(d) depicts the molecular pair having the offset π–π stacking, whereas Figure 7(e) depicts C–H···π and C···N intermolecular interaction. Thus, Hirshfeld surface analysis represents a unique approach towards an understanding of different interactions in the crystal structure and is an indispensable tool in crystal engineering.

In addition to the Hirshfeld surface analysis, the fingerprint plots also provide some quantitative information about the individual contribution of the intermolecular interaction

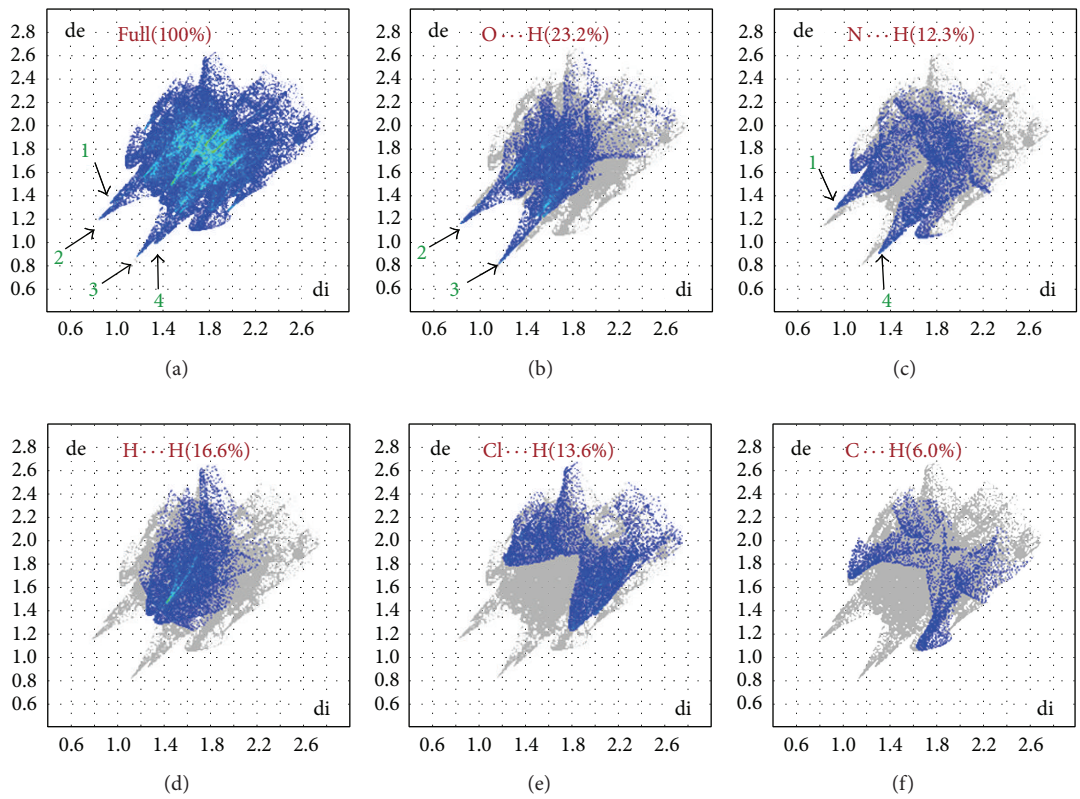

Figure 8: Fingerprint plots showing the percentage contribution of the individual types of interaction to the total Hirshfeld surface area.

in the crystal packing (Figure 8). Some distinct spikes (shown by arrows) appearing in the 2D fingerprint plot indicate the different interactions motifs in the crystal lattice. The spikes labeled by 2 and 3 are indicating the C–H···O hydrogen bond (23.2%) and the spikes labeled by 1 and 4 are indicating the C–H···N and N–H···N intermolecular interaction (12.3%). The molecular stacking, in spite of having a substantial energetic stabilization, much less contributes [C···C (4.5%)] towards the crystal packing. The remaining area of the finger print plot is occupied by H···H (16.6%) and Cl···H (13.6%) contact regions.

4. Conclusion

In summary, we have described the title compound in terms of different noncovalent interactions that govern the crystal packing. The N···C interaction imparts the maximum stabilization along with other weak intermolecular interactions in the packing. Molecular pairs with C–H···π, π–π, and N···C interactions are observed to contribute more than hydrogen bonds. We have analysed the geometrical features of the title compound. The observed molecular conformations of this molecule obtained from X-ray analysis agree well with the conformation obtained from geometrical optimization (DFT + Disp with B3LYP/6-31G**). Finally, Hirshfeld surface analysis and fingerprint plots represent a unique approach for understanding of the contribution of individual types of interaction within the crystal structure.

Conflict of Interests

The authors declare that there is no conflict of interests regarding the publication of this paper.

References

[1] H. Uneme, M. Konobe, A. Akayama, T. Yokota, and K. Mizuta, "Discovery and development of a novel insecticide "clothianidin"," *Sumitomo Kagaku*, vol. 2, pp. 20–33, 2006.

[2] K. Li and Q. X. Li, "Development of an enzyme-linked immunosorbent assay for the insecticide imidacloprid," *Journal of Agricultural and Food Chemistry*, vol. 48, no. 8, pp. 3378–3382, 2000.

[3] S. Wanatabe, S. Ito, Y. Kamata et al., "Development of competitive enzyme-linked immunosorbent assays (ELISAs) based on monoclonal antibodies for chloronicotinoid insecticides imidacloprid and acetamiprid," *Analytica Chimica Acta*, vol. 427, no. 2, pp. 211–219, 2001.

[4] H.-J. Kim, W. L. Shelver, E.-C. Hwang, T. Xu, and Q. Li, "Automated flow fluorescent immunoassay for part per trillion detection of the neonicotinoid insecticide thiamethoxam," *Analytica Chimica Acta*, vol. 571, no. 1, pp. 66–73, 2006.

[5] S. Fang, B. Zhang, K.-W. Ren, M.-M. Cao, H.-Y. Shi, and M.-H. Wang, "Development of a sensitive indirect competitive enzyme-linked immunosorbent assay (ic-ELISA) based on the monoclonal antibody for the detection of the imidaclothiz residue," *Journal of Agricultural and Food Chemistry*, vol. 59, no. 5, pp. 1594–1597, 2011.

[6] Y. J. Chen, Y. Wang, N. Li, and M. L. Gong, "Methodological study on the determination of residual pesiclde in Brassica chinensis by HPLC," *China Tropical Medicine*, vol. 9, no. 2, pp. 361–362, 2009.

[7] H. Uneme, "Chemistry of clothianidin and related compounds," *Journal of Agricultural and Food Chemistry*, vol. 59, no. 7, pp. 2932–2937, 2011.

[8] P. Jeschke, H. Uneme, J. Benet-Buchholz et al., "Clothianidin (TI435)-the third member of the chloronicotinyl insecticide (CNI) family," *Pflanzenschutz-Nachr. Bayer*, vol. 56, pp. 5–25, 2003.

[9] L. Maschio, B. Civalleri, P. Ugliengo, and A. Gavezzotti, "Intermolecular interaction energies in molecular crystals: comparison and agreement of localized Møller-Plesset 2, dispersion-corrected density functional, and classical empirical two-body calculations," *The Journal of Physical Chemistry A*, vol. 115, no. 41, pp. 11179–11186, 2011.

[10] F. Bernardi and S. F. Boys, "Counterpoise correction and basis set superposition error," *Molecular Physics*, vol. 19, article 553, 1970.

[11] R. Dovesi, V. R. Saunders, C. Roetti et al., *CRYSTAL09 (CRYSTAL09 User's Manual)*, University of Torino, Torino, Italy, 2009.

[12] M. A. Spackman and D. Jayatilaka, "Hirshfeld surface analysis," *CrystEngComm*, vol. 11, no. 1, pp. 19–32, 2009.

[13] M. A. Spackman and J. J. McKinnon, "Fingerprinting intermolecular interactions in molecular crystals," *CrystEngComm*, vol. 4, no. 66, pp. 378–392, 2002.

[14] H.-M. Liu, W. Zhang, Y. Zheng, G.-C. Ma, and W.-Q. Zhang, "Synthesis and crystal structure of *trans*-2,2′-(1,4-but-2-enediyldithio)-1,3-dithiazole and its Ag(I) complex with two-dimensional framework," *Journal of Molecular Structure*, vol. 752, no. 1–3, pp. 40–44, 2005.

[15] A. Altomare, G. Cascarano, C. Giacovazzo, and A. Guagliardi, "Completion and refinement of crystal structures with *SIR92*," *Journal of Applied Crystallography*, vol. 26, part 3, pp. 343–350, 1993.

[16] G. M. Sheldrick, "A short history of *SHELX* Program for Crystal Structure Refinement," *Acta Crystallographica A*, vol. 64, pp. 112–122, 2008.

[17] L. J. Farrugia, "*WinGX* suite for small-molecule single-crystal crystallography," *Journal of Applied Crystallography*, vol. 32, part 4, pp. 837–838, 1999.

[18] L. J. Farrugia, "*ORTEP*-3 for windows—a version of *ORTEP*-III with a graphical user interface (GUI)," *Journal of Applied Crystallography*, vol. 30, part 5, pp. 565–566, 1997.

[19] C. F. Macrae, I. J. Bruno, J. A. Chisholm et al., "*Mercury CSD 2.0*—new features for the visualization and investigation of crystal structures," *Journal of Applied Crystallography*, vol. 41, part 2, pp. 466–470, 2008.

[20] M. Nardelli, "*PARST*95—an update to *PARST*: a system of Fortran routines for calculating molecular structure parameters from the results of crystal structure analyses," *Journal of Applied Crystallography*, vol. 28, part 5, p. 659, 1995.

[21] A. L. Spek, "Structure validation in chemical crystallography," *Acta Crystallographica D: Biological Crystallography*, vol. 65, no. 2, pp. 148–155, 2009.

[22] S. K. Wolff, D. J. Grimwood, J. J. McKinnon, M. J. Turner, D. Jayatilaka, and M. A. Spackman, *Crystal Explorer (Version 3.0)*, University of Western Australia, Crawley, Australia, 2012.

[23] R. Ahlrichs, M. Baer, M. Haeser, H. Horn, and C. Koelmel, "Electronic structure calculations on workstation computers: the program system TURBOMOLE," *Chemical Physics Letters*, vol. 162, no. 3, pp. 165–169, 1989.

[24] TURBOMOLE GmbH, "TURBOMOLE V6.3 2011, a developmentof University of Karlsruhe and Forschungszentrum Karlsruhe GmbH, 1989–2007," 2011, http://www.turbomole.com/.

[25] I. Dance, "Distance criteria for crystal packing analysis of supramolecular motifs," *New Journal of Chemistry*, vol. 27, no. 1, pp. 22–27, 2003.

[26] M. Nishio, "The CH/π hydrogen bond in chemistry. Conformation, supramolecules, optical resolution and interactions involving carbohydrates," *Physical Chemistry Chemical Physics*, vol. 13, no. 31, pp. 13873–13900, 2011.

[27] M. Nishio, "The CH/π hydrogen bond: implication in chemistry," *Journal of Molecular Structure*, vol. 1018, pp. 2–7, 2012.

[28] M. Nishio, M. Hirota, and Y. Umezawa, *The CH/π Interaction, Evidence, Nature and Consequences*, Wiley-VCH, New York, NY, USA, 1998.

[29] C. R. Martinez and B. L. Iverson, "Rethinking the term "pi-stacking"," *Chemical Science*, vol. 3, no. 7, pp. 2191–2201, 2012.